Healing of Thermoplastic Polymers at an Interface under Nonisothermal Conditions

F. Yang and R. Pitchumani*

Composites Processing Laboratory, Department of Mechanical Engineering, University of Connecticut, Storrs, Connecticut 06269-3139

Received May 16, 2001; Revised Manuscript Received October 15, 2001

ABSTRACT: Fabrication of layered thermoplastic polymer products involves applying heat and pressure to contacting thermoplastic surfaces and consolidating the interface. Polymer healing, referring to the intermolecular diffusion across the interfaces of thermoplastic tape layers in intimate contact, is one of the important steps responsible for the development of interlaminar bond strength and is strongly influenced by the temperature history. While the theory for healing under isothermal conditions is well established in the literature, the available descriptions of healing under nonisothermal processing conditions lack a sound fundamental basis. In this paper, a model for the healing process under nonisothermal conditions is developed starting from a fundamental formulation of the reptation of polymer chains. Considering the temperature dependence of the welding time, the bond strength is described as a function of temperature history. It is shown that, under certain nonisothermal conditions, considerable errors could be introduced in the prediction of the healing development using the models in the literature.

1. Introduction

Processing of thermoplastics and thermoplastic composites using techniques such as tow placement, tape laying, resistant welding, and autoclave forming is governed by the principle of fusion bonding, which involves applying heat and pressure to the interface between two contacting material layers (Figure 1). The processing temperature is usually above the glass transition point (in the case of amorphous polymer) or the melting point (in the case of the semicrystalline polymer) of the materials to reduce the viscosity and mobilize the polymer molecules. The softened materials are then spread by the applied pressure, forming close contact between the adjacent layers, a process referred to as intimate contact, followed by the interdiffusion of polymer chains across the area in contact, a process referred to as healing.

The processes of intimate contact and healing are coupled in that healing can occur only across areas of the interface that are in intimate contact. While intimate contact development is a function of the applied pressure, temperature, and time, healing is mainly governed by the temperature history and time. As a result of the coupling, however, the interlaminar bond strength, σ, is a function of the processing temperature, T, the consolidation pressure, p, and the processing time, t.[1−6]

$$\sigma = f(T, p, t) \tag{1}$$

In this paper, we focus on the description of the healing process by assuming that complete intimate contact is already achieved at the interface. Description of the intimate contact process has been reported in the literature, which the reader is referred to.[4,7−9]

Healing of a polymer interface via molecular interdiffusion is a temperature-dependent process, and the reptation theory, which models the motion of individual linear polymer chains in amorphous bulk, is widely used to describe the process under isothermal conditions.[10,11] In the model, a polymer chain of length L is considered to be confined to a tube, which represents the steric effects of neighborhood chains (Figure 2). The tube forms a geometric constraint such that the chain can only move along its curvilinear length. At the beginning of the process, $t = 0$, the chain, represented by the thin solid line in Figure 2, is totally encompassed by the original tube. The chain moves within the tube in a Brownian motion manner, and after a period of time, $t = t_1$, the chain ends escape from the original tube, forming the "minor chains". The length, l, of the minor chains increases with time and reaches L at the reptation time t_R (when the entire polymer chain escapes from the tube).

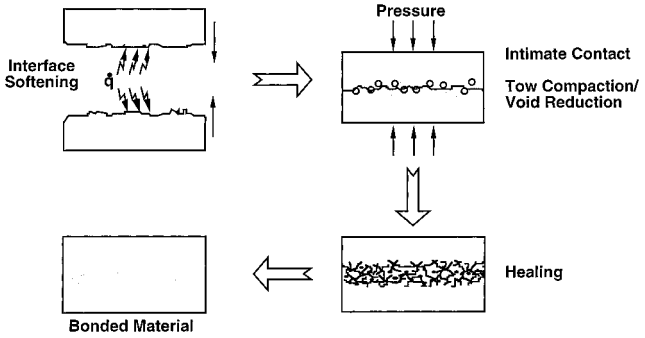

Figure 1. Schematic illustration of the steps in a fusion bonding process.

On the basis of a description of the minor chain development, the polymer molecular motion near the interface between two thermoplastic layers during the healing process is considered, as depicted schematically in Figure 3. The two layers are assumed to be in perfect contact at the interface throughout the process. Note that only the molecules on one side of the interface are illustrated for clarity. At time $t = 0$, all the minor chains have zero length as denoted by the dots in Figure 3. As time proceeds, the lengths of the minor chains grow, and

* To whom correspondence should be addressed.

10.1021/ma010858o CCC: $22.00
Published on Web 03/15/2002

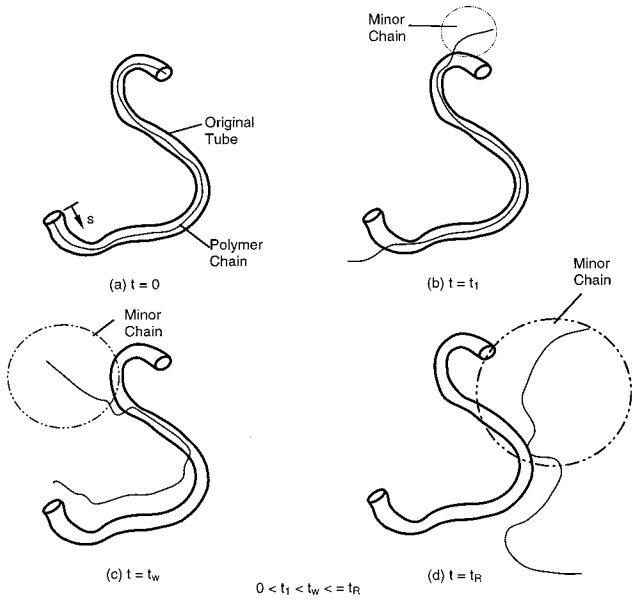

Figure 2. Reptation movement of a linear polymer chain in an entangled melt. The chain escapes from its original tube at the reptation time, t_R, and the maximum bond strength is achieved at the welding time, t_w ($\leq t_R$).

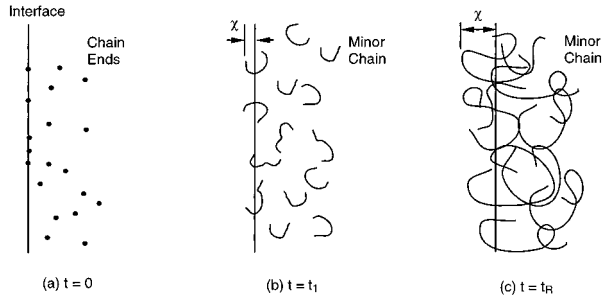

Figure 3. Interdiffusion of minor chains across a polymer−polymer interface. The polymer layers are assumed to be in complete intimate contact and only the molecules on one side of the interface are shown for clarity (illustrations redrawn from ref 1).

some of the chains move across the interface with an interpenetration distance, χ (Figure 3), which contributes to the bond strength buildup. After the reptation time, the interpenetration and entanglement of all the polymer chains are fully developed and the molecular configuration at the interface is identical to that of the virginal bulk material. The bond strength, σ, is proportional to the interpenetration distance χ, which is related to the minor chain length as $\chi \sim \sqrt{l}$ by considering the minor chains to amble across the interface via a random walk motion.[2] The ultimate bond strength, σ_∞, is achieved as the interpenetration depth and the minor chain length reach their maximum values, χ_∞ and L, respectively. A degree of healing may be defined as the ratio of the instantaneous interfacial bond strength to the ultimate bond strength as[10,11]

$$D_h(t) = \frac{\sigma}{\sigma_\infty} = \frac{\chi}{\chi_\infty} = \left(\frac{l}{L}\right)^{1/2} \tag{2}$$

The above equation is obtained by assuming that the factor of proportionality of the strength with the square root of minor chain length is the same for $\sigma(t)$ and σ_∞. Note that eq 2 applies to isothermal and nonisothermal conditions alike; however, the growth of the minor chain length with time depends on the temperature history.

The evolution of l with time is governed by a diffusion process of polymer chains. Under isothermal conditions, in which the diffusion coefficient for a given polymer chain is likely to be a constant, the increase in the minor chain length, l, for time $t < t_R$ is expressed as[1,10]

$$\frac{l}{L} = \left(\frac{t}{t_R}\right)^{1/2} \tag{3}$$

where t_R is the reptation time when the entire polymer chain has diffused out of the tube. From eqs 2 and 3 it follows that, under isothermal conditions, the degree of healing is given by

$$D_h(t) = \frac{\sigma}{\sigma_\infty} = \left(\frac{t}{t_R}\right)^{1/4} \tag{4}$$

The reptation time, t_R, a function of temperature, may be described by an Arrhenius type equation[5] or other empirical means.[4] It must be pointed out that the scaling relationships $l \sim t^{1/2}$ and $\sigma \sim t^{1/4}$ are not always valid, depending on the time scale, and the initial configuration of the chain ends at the interface, etc. For example, if the chain ends are not initially concentrated at the interface, or in the case of $t > t_R$, the bond strength may follow $\sigma \sim t^{1/2}$.[2,12,13]

Bastien and Gillespie[14] extended the reptation theory to nonisothermal fusion bonding of amorphous thermoplastic laminates. In their model development, the temporal domain of a nonisothermal healing process was divided into q time intervals ($t_{i+1} - t_i = \Delta t = t/q$), and the process in each ith interval was considered to be isothermal at the average of the temperatures between t_i and t_{i+1}. The incremental bond strengths accrued within each Δt were derived from the isothermal reptation theory and the intent of the model was to determine the bond strength at any instant t as the summation of the incremental values. Bastien and Gillespie reported two nonisothermal healing models by postulating two extensions of the isothermal degree of healing expressions as follows. First, starting from eq 3, the incremental growth of the minor chain length, Δl, during the isothermal interval (t_i, t_{i+1}) was obtained as

$$\frac{\Delta l}{L} = \frac{{t_{i+1}}^{1/2} - {t_i}^{1/2}}{{t_R^*}^{1/2}} \tag{5}$$

where the reptation time t_R^* is evaluated at the average temperature, T_i^*, within the time interval. The degree of healing at a given time t was then evaluated using eqs 2 and 5 as follows.

$$D_h = \frac{\sigma}{\sigma_\infty} = \left(\frac{l}{L}\right)^{1/2} = \left[\sum_{i=0}^{t/\Delta t}\left(\frac{{t_{i+1}}^{1/2} - {t_i}^{1/2}}{{t_R^*}^{1/2}}\right)\right]^{1/2} \tag{6}$$

In a second model by Bastien and Gillespie,[14] starting from eq 4, the strength increment $\Delta\sigma$ in the time interval (t_i, t_{i+1}) was directly given as

$$\frac{\Delta\sigma}{\sigma_\infty} = \frac{{t_{i+1}}^{1/4} - {t_i}^{1/4}}{{t_R^*}^{1/4}}$$

and the degree of healing evolution with time was

determined by a summation of the incremental strength values.

$$D_h(t) = \frac{\sigma}{\sigma_\infty} = \sum_{i=0}^{t/\Delta t} \left[\frac{{t_{i+1}}^{1/4} - {t_i}^{1/4}}{{t_R^*}^{1/4}} \right] \tag{7}$$

Since eqs 6 and 7 are purely mathematical extensions based on the same assumptions and derivation method except using different equations in the reptation theory as starting points, there is no strong physical justification supporting either expression. Bastien and Gillespie resorted to experiments and concluded that eq 7 was more appropriate, since it better matched their experimental data.

The foregoing nonisothermal extension of the healing model seemingly appears plausible and in fact has been widely accepted and used in modeling fabrication processes.[5,6,15] However, a closer examination of the model reveals that the expression reported for the incremental bond strengths during each *i*th time interval, i.e., the term within square brackets in eq 7, is truly valid only if the process were isothermal at the average temperature T_i^* from $t = 0$ to $t = t_{i+1}$, for each *i*. Since this does not represent the thermal history during actual processing conditions, the model is strictly inappropriate for a nonisothermal process.

Sonmez and Hahn[16] modified the isothermal reptation model using an approach similar to that of Bastien and Gillespie in order to simulate nonisothermal healing during thermoplastic composite tape placement. Differentiating eq 3 with respect to time, the increase in the minor chain length with time was given as[16]

$$\frac{dl}{L} = \frac{dt}{2\sqrt{t_R t}} \tag{8}$$

Integrating the above equation, and recalling that $\sigma \sim \sqrt{l}$, the following expression was reported for the interfacial bond strength as a function of the nonisothermal history.

$$D_h(t) = \frac{\sigma}{\sigma_\infty} = \sqrt{\frac{l}{L}} = \left[\int_0^t \frac{d\tau}{2\sqrt{\tau t_R(\tau)}} \right]^{1/2} \tag{9}$$

The above integral has a similar drawback as that in the case of the Bastien and Gillespie model. When applying eq 8 to a nonisothermal process at the time interval $(\tau, \tau + d\tau)$, the integrand in eq 9 is only appropriate if the process were isothermal with the reptation time $t_R(\tau)$ from $t = 0$ to $t = \tau$. Again, this does not represent the real temperature history.

The development of the above nonisothermal healing models also ignored an important limitation when using the reptation theory, eqs 2−4. As pointed out by Wool and coauthors,[1,2,17] these equations are only valid for low molecular weights, *M*, in the range of $M_c < M < 8M_c$, where M_c is the critical entanglement molecular weight. However, for typical engineering thermoplastics, the molecular weight range is $M > 8M_c$, and eqs 2−4 are not applicable. At high molecular weights, the interpenetration depth and the minor chain length do not have to reach χ_∞ and *L* to obtain the maximum bond strength, σ_∞, which is achieved instead at the welding time, t_w ($< t_R$, as shown in Figure 2c), at which χ and *l* have the values of χ_w ($< \chi_\infty$) and L_w ($< L$), respectively. On the basis of the above consideration, a more general expression of the degree of healing is obtained using the parameters at the welding time as follows:

$$D_h(t) = \frac{\sigma}{\sigma_\infty} = \frac{\chi}{\chi_w} = \left(\frac{l}{L_w}\right)^{1/2} = \left(\frac{t}{t_w}\right)^{1/4} \tag{10}$$

Note that the above equation is valid for the full range of molecular weight because of the fact that in the low molecular weight range, $t_w = t_R$, $\chi_w = \chi_\infty$, $L_w = L$, and eq 10 reduces to the expression given by eq 4. On the basis of the same reasoning, it is more appropriate to replace the reptation time, t_R, in the models of Bastien and Gillespie (eq 7) and Sonmez and Hahn (eq 9) by the welding time, t_w.

It is evident from the foregoing discussion that more research is needed to describe polymer healing under nonisothermal conditions usually encountered in processing. The intent of the present study is to address this critical issue by developing a fundamental description of nonisothermal healing, founded on a first-principles formulation of the polymer reptation process. Starting from a description of the Brownian motion of a single polymer chain, an analytical relationship is derived to relate the bond strength evolution to the nonisothermal temperature history. The model development is discussed in the next section. Parametric studies are presented to illustrate the effects of the temperature history on the healing development. Comparisons with the expressions of Bastien and Gillespie[14] and of Sonmez and Hahn[16] are presented to examine the accuracy of the models in the literature relative to the exact solution. The model is validated using experimental data on the fusion bonding of AS4/PEEK and AS4/PEKK, over several nonisothermal conditions.

2. The Nonisothermal Healing Model

As in the studies of isothermal healing development, we start with a description of the reptation motion of a polymer chain encased in a surrounding tube. A probability density function, $P(s, t)$, is defined as the probability of finding a particular chain segment at some position *s* at time *t*, where *s* is the curvilinear coordinate along the encompassing tube (Figure 2a). The density function $P(s, t)$ was determined through a random walk analysis of the chain segments in the tube and was shown to be mathematically governed by a diffusion equation[10,11,18]

$$\frac{\partial P}{\partial t} = D \frac{\partial^2 P}{\partial s^2} \tag{11}$$

where *D* is the reptation (or curvilinear) diffusion coefficient corresponding to the back and forth movements of the polymer chain in the confining tube. Generally, the diffusivity *D* depends on a number of factors such as the molecular weight, *M*, molecular weight distribution, temperature, *T*, concentration, *c*, and hydrostatic pressure, *p*.[19,20] In this paper, we only consider the influence of the temperature and its time variation, while the contribution of the other parameters (e.g., *M*, *c*, *t*) will be discussed in a future work. In the current study, the reptation diffusion coefficient, *D*, is treated as a constant for isothermal healing whereas, in the nonisothermal case, *D* is time variant through its dependence on the temperature.

At time $t = 0$, the chain segment considered is at the origin, $s = 0$, and the initial condition associated with eq 11 may be written as

$$P(s, 0) = \delta(0) \tag{12}$$

where δ is the Dirac delta function. The diffusion domain is considered to be infinitely large ($|s| \rightarrow \infty$), and since the chain segment will never be able to move across an infinite distance, the following natural boundary conditions must be automatically satisfied

$$P(s, t) = 0; \frac{\partial P(s, t)}{\partial s} = 0 \quad \text{as} \quad |s| \rightarrow \infty \tag{13}$$

Under isothermal conditions ($T = T_0$), the reptation diffusivity $D_0 = D(T_0)$ is a constant, and the solution of eqs 11 and 12 is given as[11,18]

$$P(s, t) = \frac{1}{[4\pi D_0 t]^{1/2}} \exp[-s^2/4D_0 t] \tag{14}$$

The mean-square displacement of the polymer chain at time t corresponds to the square of the minor chain length $l^2(t)$ and may be evaluated as follows using the isothermal probability density function (eq 14).

$$\langle s^2 \rangle = l^2 = \int_{-\infty}^{+\infty} s^2 P(s, t)\, \mathrm{d}s = 2D_0 t \tag{15}$$

Recall that the welding time for a given temperature is defined as the time required for the minor chain length to reach L_w, at which point the maximum bond strength is obtained. From eq 15, we may write

$$t_w(T_0) = \frac{{L_w}^2}{2D_0} \tag{16}$$

Evidently, the one-fourth power variation of the degree of healing with time under isothermal conditions, eq 10, follows from eqs 15 and 16.

For an arbitrary temperature history, $T(t)$, the reptation diffusivity is a function of time, $D(t)$, and the nonisothermal bond strength evolution with time is obtained as solution of the governing equation, eq 11, with a variable coefficient, and the associated conditions (eqs 12 and 13). The system of equations may be solved using the separation of variables technique,[21] or using Fourier transformation, as presented in the following discussion.

A Fourier transformation of eq 11 with respect to s, subject to the natural boundary conditions (eq 13) yields

$$\frac{\mathrm{d}\hat{P}}{\mathrm{d}t} = -D(t)\omega^2 \hat{P} \tag{17}$$

where ω is the transformed variable in the frequency domain, and $\hat{P}$ denotes the Fourier transformation of the probability density function $P(s, t)$, defined as

$$\hat{P}(\omega, t) = \frac{1}{\sqrt{2\pi}} \int_{-\infty}^{+\infty} P(s, t) \exp(-i\omega s)\, \mathrm{d}s \tag{18}$$

Notice that the diffusivity, a function of time, $D(t)$, for a nonisothermal process is a constant with respect to the transformation in eq 17. The solution of the first-order ordinary differential equation, eq 17, is given by

$$\hat{P}(\omega, t) = \hat{P}_0 \exp[\int_0^t -D(t)\omega^2\, \mathrm{d}t] \tag{19}$$

where using a Fourier transformation of the initial condition, eq 12,

$$\hat{P}_0 = \hat{P}(\omega, 0) = \frac{1}{\sqrt{2\pi}}$$

An inverse Fourier transformation of $\hat{P}(\omega, t)$ given by eq 19 yields the probability density function $P(s, t)$ in the original domain:

$$P(s, t) = \frac{1}{\sqrt{2\pi}} \int_{-\infty}^{+\infty} \hat{P}(\omega, t) \exp(i\omega s)\, \mathrm{d}\omega = \frac{1}{2\pi} \int_{-\infty}^{+\infty} \exp[\int_0^t -D(t)\omega^2\, \mathrm{d}t][\cos(\omega s) + i \sin(\omega s)]\, \mathrm{d}\omega \tag{20}$$

In the above transformation, the imaginary term drops to zero because of the fact that an odd function, $\sin(\omega s)$, is integrated over a symmetric interval $(-\infty, +\infty)$, and the probability density function is obtained as

$$P(s, t) = \frac{1}{2\pi} \int_{-\infty}^{+\infty} \exp[\omega^2 \int_0^t -D(t)\, \mathrm{d}t] \cos(\omega s)\, \mathrm{d}\omega \tag{21}$$

Equation 21 forms the basis for nonisothermal healing analysis. It may be verified that for isothermal healing, eq 14 is recovered by setting $D(t) = D_0 = constant$ in eq 21 and evaluating the resulting integrals.

Equation 16, which relates the welding time to the reptation diffusivity at any temperature, T, is used to replace the diffusion coefficient, $D(t)$, in terms of the welding time in eq 21, as $D(t) = {L_w}^2/2t_w[T(t)]$. Furthermore, defining $f(t)$ for brevity as

$$f(t) = \int_0^t \frac{1}{2t_w}\, \mathrm{d}t \tag{22}$$

the probability distribution function $P(s, t)$ (eq 21) is evaluated as follows.

$$P(s, t) = \frac{1}{\sqrt{2\pi}} \int_{-\infty}^{+\infty} \exp[-f(t)\, {L_w}^2\, \omega^2] \cos(\omega s)\, \mathrm{d}\omega = \frac{1}{\sqrt{4\pi f(t) {L_w}^2}} \exp[-s^2/4f(t){L_w}^2]$$

Following eq 15, the square of the minor chain length at time t for a nonisothermal temperature history is determined using the probability density function as

$$l^2(t) = \int_{-\infty}^{+\infty} s^2 P(s, t)\, \mathrm{d}s = \int_{-\infty}^{+\infty} s^2 \frac{1}{\sqrt{4\pi f(t) {L_w}^2}} \exp[-s^2/4f(t){L_w}^2]\, \mathrm{d}s = 2f(t){L_w}^2 \tag{23}$$

From eqs 10, 22, and 23, the nonisothermal degree of healing evolution with time is given by the following expression

$$D_h(t) = \left(\frac{l}{L_w}\right)^{1/2} = [2f(t)]^{1/4} = \left[\int_0^t \frac{1}{t_w(T)}\, \mathrm{d}t\right]^{1/4} \tag{24}$$

The foregoing result is based on the solution of the

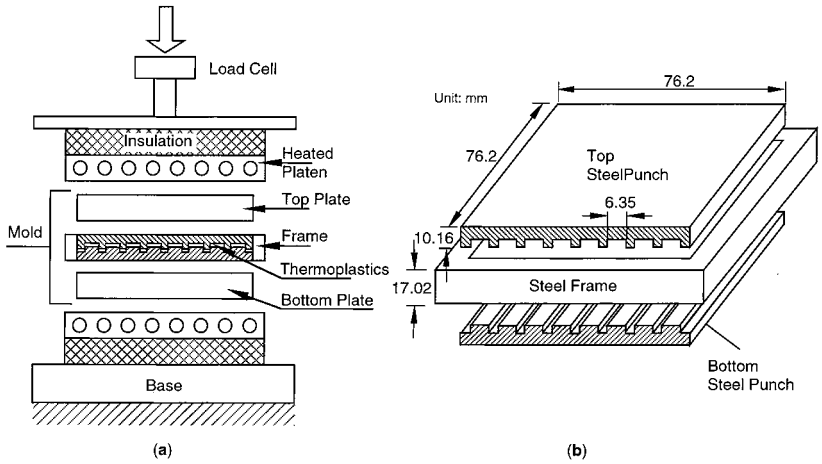

Figure 4. (a) Schematic of the fabrication setup used and (b) a view of the mold used to prepare the lap shear specimens.

Table 1. Properties of the Polymers Used in the Experimental Studies

polymer	glass transition point, T_g (°C)	melting point, T_m (°C)
PEEK	143	338
PEKK	139	330

fundamental equations governing reptation dynamics, without any further assumptions or an ad hoc formulation, and therefore, it constitutes a rigorous model for nonisothermal healing. For a given temperature history, and the temperature dependence of the welding time, the degree of healing can be evaluated using eq 24. Note that, for a constant temperature healing process, $t_w(T)$ is a constant, and the degree of healing reduces to the expression for isothermal healing given by eq 10.

3. Experimental Studies

Experimental studies consisting of fabrication and testing of lap shear specimens were conducted with the primary objective of validating the nonisothermal healing model presented in the previous section. The composite materials used in this study were AS4 carbon fibers reinforcing poly(ether−ether−ketone) (PEEK) thermoplastic (referred to as AS4/PEEK), and AS4 carbon fibers reinforcing poly(ether−ketone−ketone) (PEKK) thermoplastic (referred to as AS4/PEKK) prepreg ribbons, each with a thickness of 0.178 mm and a width of 6.35 mm, available from Cytec Fiberite, Inc. The volume fraction of the AS4 carbon fibers in AS4/PEEK was 58.5% and 56% in the case of AS4/PEKK. The glass transition temperature and melting point of the thermoplastic polymers PEEK and PEKK, as provided by the manufacturer, are given in Table 1. A programmable Tetrahedron hot press, schematically shown in Figure 4a, was used in the fabrication of lap shear samples. The press has two 254 × 254 mm platens with a force capacity of 5 tons and maximum temperature of 455 °C. A steel mold with grooves to contain the thermoplastic ribbons was used in the experiments. The top punch consisted of eight rectangular grooves and the bottom punch had eight mating rectangular teeth. This mold configuration provided for fabrication of eight lap shear samples under the same processing conditions in one run. The width of the grooves was designed to be the same as that of the specimens so that the walls can be used to prevent outflow of bulk resin.

The thermoplastic prepreg ribbons were cut and placed in the grooves for making lap shear specimens as depicted in Figure 5. The ribbons to be bonded were cleaned with acetone, and care was taken to prevent the specimen surfaces from being contaminated. Further, to prevent the specimens from sticking to the mold, aluminum foil was used between the specimens and the grooves. The mold was placed in the Tetrahedron hot press, which was programmed to yield the temperature schedules of the form in Figure 6. The temperature schedules begin with a linear ramp from T_0 to T_f within t_{ramp} seconds, followed by a hold stage with a constant temperature T_f (Figure 6).

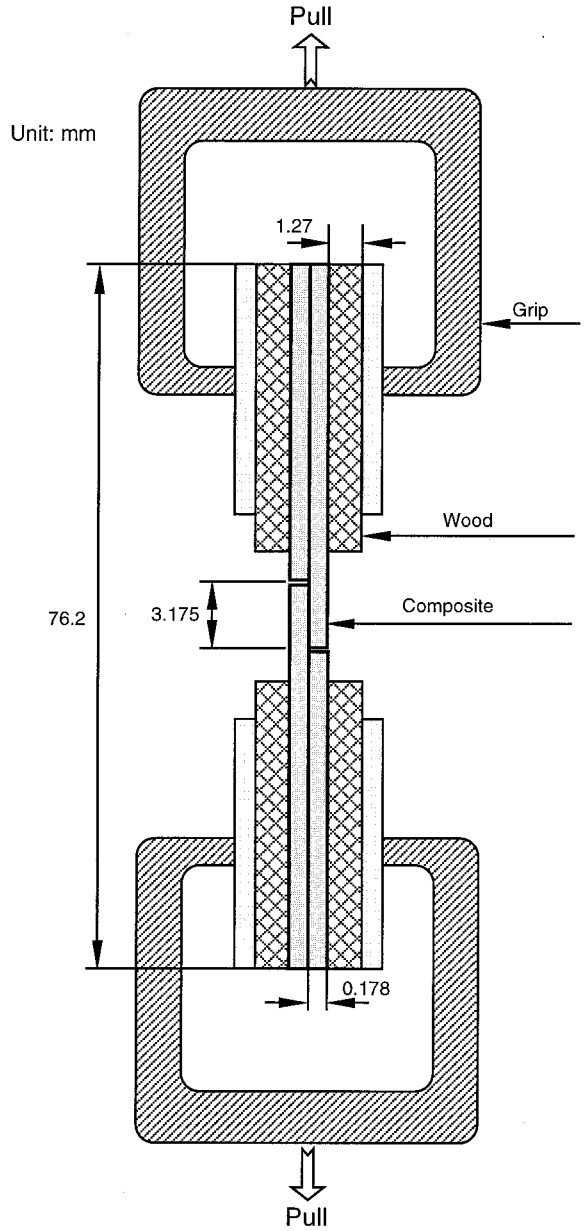

Figure 5. Layout and dimensions of the lap shear specimens.

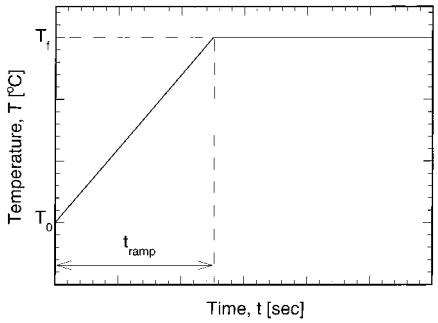

Figure 6. Schematic of the profile of the temperature variation used in the parametric and model comparison studies and in the experimental validation of the nonisothermal healing model. Specific values of the parameters of the temperature schedules used in the studies are summarized in Tables 2 and 3.

Table 2. Thermoplastic Materials and Values of the Parameters of the Temperature Schedules (Figure 6) Used in the Model Validation Studies (Figures 12 and 13)

test	material	T_0 (°C)	T_f (°C)	t_{ramp} (s)
1	AS4/PEEK	370	400	250
2	AS4/PEEK	370	400	2500
3	AS4/PEEK	370	400	5500
4	AS4/PEKK	365	395	350
5	AS4/PEKK	365	395	3500
6	AS4/PEKK	365	395	5500

The three parameters in the ramp−hold temperature schedules used in the experimental studies are tabulated in Table 2. Specimens were fabricated for several different bonding times within each schedule. The amount of pressure needed to ensure intimate contact between thermoplastic layers was calculated using the intimate contact models in refs 8 and 9. It was found that a load of 908 kg was sufficient for the layers to achieve complete intimate contact within 10 s in all the cases. At the end of the desired fusion bonding time, the mold was taken out of the hot press and quenched in cold water.

The bonded specimens were tested at room temperature with an Instron machine operating in tension mode. A crosshead speed of 12.7 mm/min was used in this study. Twenty four replicates were tested for each set of processing conditions. The shear strength was calculated as the fracture load divided by the lap area. The ultimate bond strengths were determined by using long enough bonding time and were found to be 64 and 66.7 MPa for AS4/PEEK and AS4/PEKK, respectively. A similar value of σ_∞ for AS4/PEEK was reported in the literature.[22] The degree of healing values were obtained as the ratio of instantaneous shear strength to the ultimate shear strength for each material.

To evaluate the model in eq 24, the information on welding time, $t_w(T)$ is needed. To the authors' knowledge, since the welding time of AS4/PEKK is not available in the open literature, it was measured experimentally following the approach given by Lee and Springer.[4] Lap shear specimens of AS4/PEKK were fabricated at *isothermal* conditions of 370, 380, and 390 °C, and several different processing times. For each sample, shear strengths were evaluated using the experimental testing procedure described previously. In each case, the time for development of complete intimate contact at the interface (about 10 s maximum) was much less than the healing time. The measured strength values therefore correlate closely to the healing process. The measured interlaminar shear strength values were converted to degree of healing by scaling with respect to the maximum strength of 66.7 MPa. The degree of healing data for each temperature were then plotted against $t^{1/4}$, since D_h exhibits a linear relationship with $t^{1/4}$ as per the isothermal reptation theory eq 4. Figure 7 shows the measured D_h values along with their respective error bars for the three isothermal temperatures

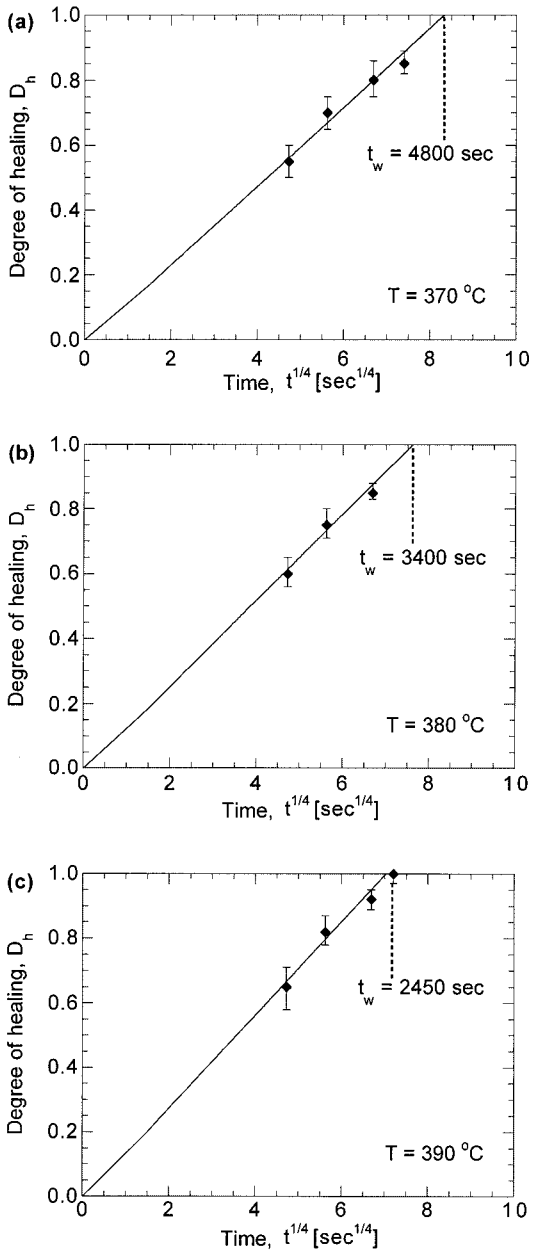

Figure 7. Measurements of the welding time of AS4/PEKK at isothermal conditions of (a) 370, (b) 380, and (c) 390 °C.

considered. The solid line denotes a best linear regression fit of the data. Note that the best fit line passes through the origin since the degree of healing is zero at the start of each process. The welding time is obtained from the slope of the linear variations, which equals $t_w^{-1/4}$, or equivalently, from the intercept of the line with $D_h = 1$, which equals $t_w^{1/4}$. The welding time values at the three temperatures are indicated in the plots and were fit to an Arrhenius relationship with temperature (in kelvin) of the form below. The empirically determined constants for AS4/PEKK are also indicated.

$$t_w = A \exp\left[\frac{E}{R}\left(\frac{1}{T} - \frac{1}{T_{ref}}\right)\right]; \quad A = 4624 \text{ s}, \quad E = 10^5 \text{ kJ/kmol}, \quad R = 8.314 \text{ kJ/kmol·K}, \quad T_{ref} = 643 \text{ K} \quad (25)$$

Lee and Springer implemented the above procedure to determine what they referred to as the *reptation* time of AS4/PEEK. However, on the basis of the nature of the procedure used in their study, it appears that the measurements are essentially

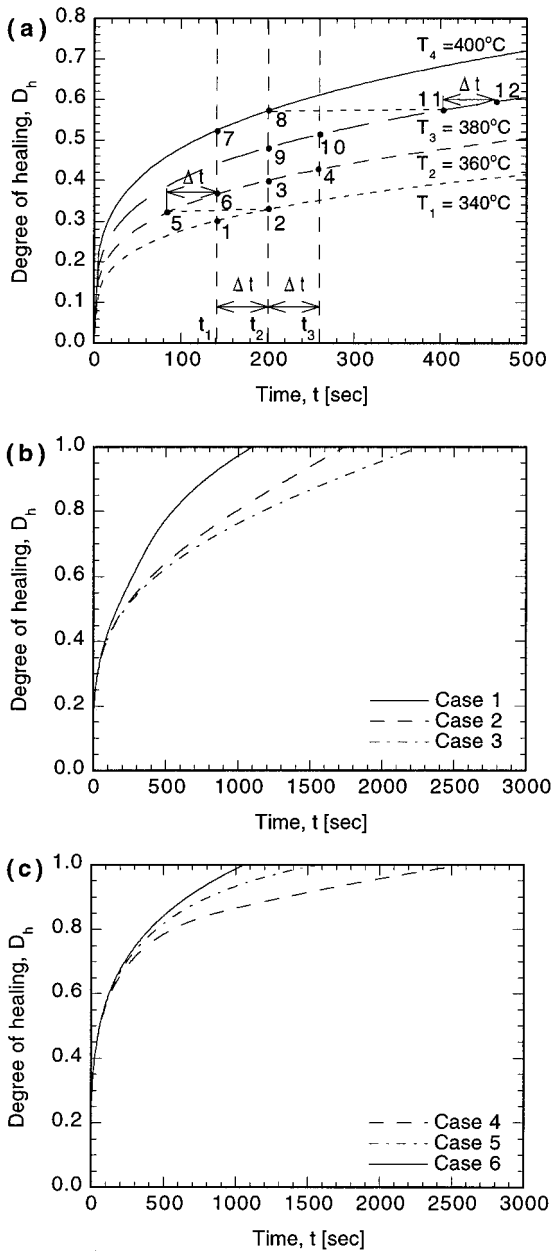

Figure 8. Parametric studies showing the effects of the temperature and temperature gradient on the healing development, for (a) constant temperatures and (b) heating and (c) cooling of AS4/PEEK samples. The case numbers pertain to the temperature profiles in Figure 6.

the *welding* time, whose temperature dependence is given by the expression below.[4]

$$t_w = \left(\frac{1}{44.1}\exp\frac{3810}{T}\right)^4 \tag{26}$$

4. Results and Discussion

The nonisothermal model, eq 24, was implemented numerically to predict the degree of healing as a function of time. The numerical integration is carried out until the degree of healing reaches a value of unity, or until the specified temperature cycle is complete, whichever happens first. Furthermore, the healing mechanisms are active only as long as the material temperature is above the glass transition point in the case of amorphous polymers or the melting point in the case of the semicrystalline polymers. Once a degree of healing of unity is achieved, the state of complete healing is preserved regardless of the further temperature variation.

Table 3. Thermoplastic Materials and Values of the Parameters of the Temperature Schedules (Figure 6) Used in the Parametric and Model Comparison Studies (Figures 8−10)

case	material	T_0 (°C)	T_f (°C)	t_{ramp} (s)
1	AS4/PEEK	380	420	360
2	AS4/PEEK	380	420	1800
3	AS4/PEEK	380	420	3600
4	AS4/PEEK	420	380	900
5	AS4/PEEK	420	380	1800
6	AS4/PEEK	420	380	5400
7	AS4/PEEK	340	400	500
8	AS4/PEEK	400	340	500
9	NCS/PEI	250	270	500
10	NCS/PEI	270	250	10

A parametric study was conducted to illustrate the influence of temperature history on the development of the healing process. The temperature dependence of the welding time in eq 24 and of the reptation times in eqs 7 and 9 are chosen to be that of the welding time of AS4/PEEK given in eq 26. The choice of a single expression for the welding or reptation times serves as a common basis for the purpose of the parametric studies. Figure 8a shows the degree of healing development with time predicted by the model at isothermal conditions. In all the cases, the degree of healing monotonically increases with time, and the time for achieving 100% degree of healing increases when the temperature decreases, as physically expected. It is worth noting that the predictions are identical to those of the isothermal reptation theory, which can be understood by the fact that eq 24 is identical to eq 10 at isothermal conditions. The healing development follows the relationship $D_h \sim t^{1/4}$ for all the temperatures. The dotted lines and the points identified in Figure 8a will be referred to in a later discussion.

The influence of the temperature gradient on the healing development is shown in Figure 8, parts b and c. The temperature profiles used in each case follow the ramp-and-hold variation depicted in Figure 6 and the values of T_0, T_f, and t_{ramp} are tabulated in Table 3. The effect of positive temperature ramps ($dT/dt > 0$) where the temperature is increased from 380 to 420 °C in three different time durations, identified as cases 1−3 in Table 3, is illustrated in Figure 8b. Since the welding time decreases with increasing temperature, the healing development is accelerated with a steeper ramp. Consequently, as the temperature gradient increases from cases 3 to 1, the total time for achieving complete healing (i.e., $D_h = 1$) is seen to decrease in Figure 8b. Figure 8c shows the effect of negative temperature ramps on the healing development. Again, the corresponding temperature history for each case is given in Table 3. Following a similar reasoning, as for the heating cycles, the nature of the temperature dependence of the welding time implies that a negative temperature ramp *decelerates* the healing process. This is evident in Figure 8c, which shows that the time for realizing a given degree of healing decreases as the absolute value of the negative ramp decreases from cases 4 to 6.

In addition to the parametric study, the nonisothermal healing model was compared with the models presented by Bastien and Gillespie[14] and by Sonmez and Hahn,[16] with the objective of ascertaining their accuracy

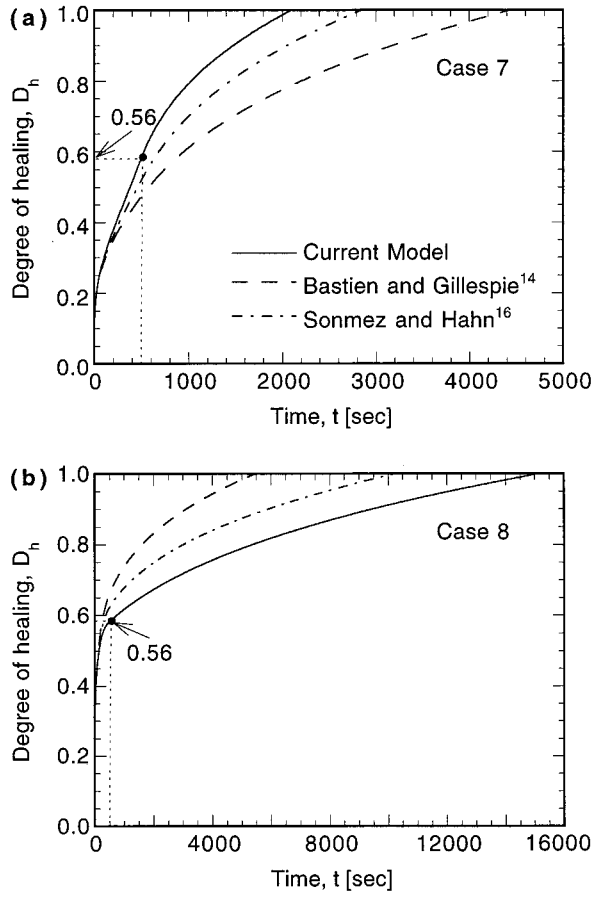

Figure 9. Comparison of the nonisothermal model (eq 24) with the models in the literature, for AS4/PEEK. Plots represents the degree of healing development for a heating cycle (plot a), and a cooling cycle (plot b).

relative to the exact model developed in this study. First, it is noted that all the nonisothermal models converge to the reptation model in eq 10 under isothermal conditions, whereas the predictions of the models are not identical under nonisothermal conditions. For the temperature histories considered in this paper, a time step of 0.1 s was found to yield converged numerical predictions for all the models. Figure 9 compares the predictions of the different healing models using the welding time of AS4/PEEK given by Lee and Springer.[4] The temperature histories used in the calculations presented in Figure 9, parts a and b, are, respectively, those of cases 7 and 8, quantified in Table 3. Case 7 corresponds to a steady heating from the melting point of AS4/PEEK (340 °C) to the maximum temperature of 400 °C with a ramp time of 500 s and holding the temperature at 400 °C until complete healing is attained.

It is seen in the initial stages of the process that all the models are comparable in predicting the healing development. However, beyond about 30% healing, the models diverge in their estimate of the degree of healing. In particular, the model of Bastien and Gillespie predicts a considerably slower evolution of healing at the interface. The reason for the error introduced can be conceptually explained using Figure 8a as an illustration. Consider two consecutive time steps t_1-t_2 (with average temperature T_1) and t_2-t_3 (with average temperature T_2) in Bastien and Gillespie's model. At the first time step, the degree of healing increment is that between points 1 and 2 on the $T = T_1$ curve; at the next time step, Bastien and Gillespie's model predicts the increment from points 3 to 4 on the $T = T_2$ curve. However, as we mentioned before, this increment is only valid if the temperature were T_2 from $t = 0$ to point 4. An appropriate increment is possibly between points 5 (having the same degree of healing as point 2) and 6 on the $T = T_2$ curve, since the increment should be based on the interpenetration (or degree of healing) value at the end of the first step. Clearly, the actual increment is larger than that used in Bastien and Gillespie's prediction; hence the slower evolution of healing. The Sonmez and Hahn model also yields a smaller degree of healing at any instant during the process, although the deviation from the exact solution is less than that for the Bastien and Gillespie model. The error introduced by Sonmez and Hahn's model can also be explained in a similar manner as above since the model is but a continuous representation of Bastien and Gillespie's discrete model. For the temperature cycle considered, the welding time is significantly overestimated by more than a factor of 2 in the case of the Bastien and Gillespie model, and by about 33% in the case of the model of Sonmez and Hahn.

Figure 9b shows the comparison for a cooling schedule with a negative ramp denoted by case 8 in Table 3. The relative trend among the models is converse to that seen in the case of the heating schedule in Figure 9a. The model of Bastien and Gillespie and that of Sonmez and Hahn overpredict the healing development rates, with the welding times being 5500 and 10 000 s, respectively, in comparison to the value of 15 000 s predicted by the exact solution. The overpredictions may be explained following a similar reasoning as above, by considering the time intervals from t_1 to t_2 and from t_2 to t_3 in Figure 8a, but now focusing on a cooling from an average temperature of T_4 during the first interval ($t_1 \rightarrow t_2$) to T_3 in the interval $t_2 \rightarrow t_3$. It is evident that the model of Bastien and Gillespie uses the healing increment from points 7 to 8 during the first time interval and that from points 9 to 10 during the second, instead of from points 11 to 12 as would be expected from the viewpoint of continuity of the degree of healing. The magnitude of the increments used in the Bastien and Gillespie model (for example between points 9 and 10) are larger than the actual (for example, between points 11 and 12), which is reflected in the overprediction on the degree of healing evolution.

It is interesting to note from Figure 9, parts a and b that the degree of healing at the end of the linear ramp portions of the schedules, i.e., at $t = 500$ s, are identical (as marked in the plots) regardless of whether the material is heated from 340 to 400 °C in 500 s or cooled from 400 to 340 °C in 500 s. This is physically expected since the material is subject to the same temperature values except for the time during the linear schedule when the temperature is experienced. Furthermore, this constitutes an important distinction with respect to the other models which incorrectly predict a lower degree of healing at the end of a heating ramp and a higher degree of healing at the end of a cooling ramp. The models in the literature are therefore inconsistent with the physical healing process under nonisothermal conditions.

Further comparison among the models is presented for the thermoplastic composite, BASF commingled PEEK/graphite NCS woven fabric using a poly(ether imide) (PEI) film at the interface (denoted as NCS/PEI).

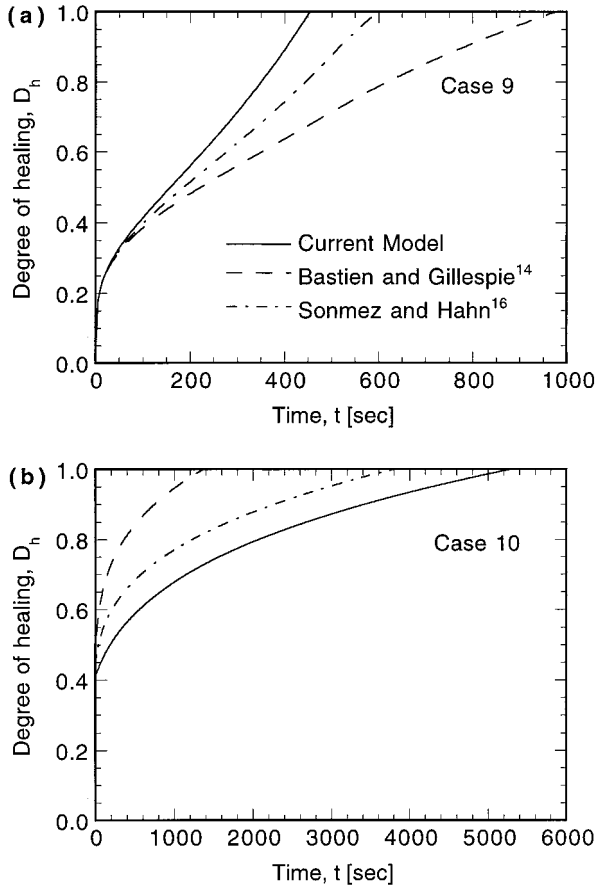

Figure 10. Comparison of the nonisothermal model (eq 24) with the models in the literature, for NCS/PEI. Plots represent the degree of healing development for a heating cycle (plot a), and a cooling cycle (plot b).

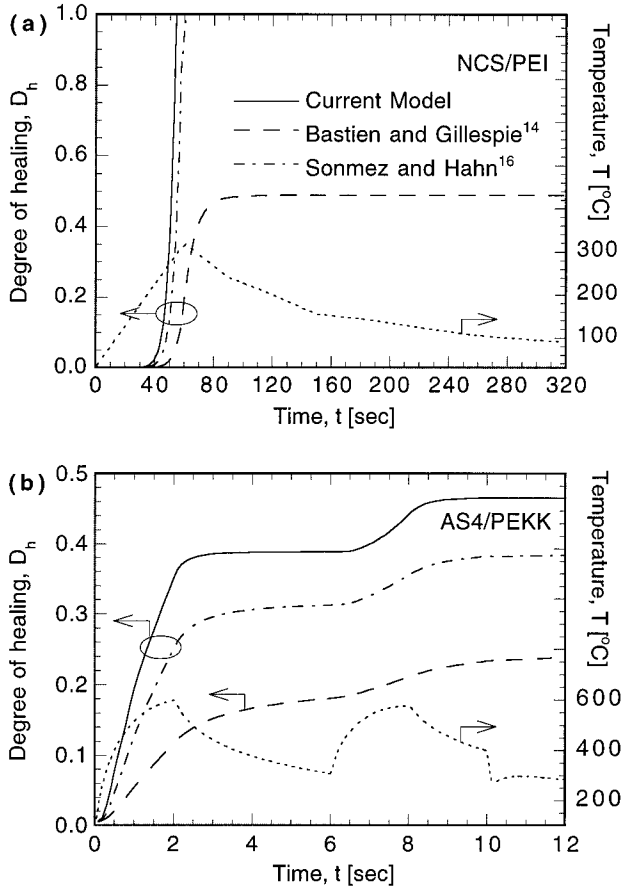

Figure 11. Comparison of the nonisothermal model (eq 24) with the models in the literature, for NCS/PEI and AS4/PEEK under actual processing conditions: (a) degree of healing development in NCS/PEI for a resistance welding temperature history[14] and (b) degree of healing evolution in AS4/PEKK for a thermal history encountered in a tow−placement process.[5]

For this material, the welding time expression as a function of temperature was given by Bastien and Gillespie.[14] Figure 10, following the same presentation format as in Figure 9, shows the comparison results for a heating ramp, case 9 (Table 3), in Figure 10a, and for a cooling ramp, case 10 (Table 3), in Figure 10b. Case 9 corresponds to a linear increase in temperature from 250 to 270 °C, in 500 s. Unlike the plots in Figure 9a, where the healing rates are seen to decrease monotonically in all the models, the healing rates in Figure 10a exhibit an increase in the later stages of temperature schedule. This is particularly evident in the present model and in the model by Sonmez and Hahn. The observed trend can be explained by the fact that welding time of ACS/PEI reduces sharply from 5446 s at 250 °C to 81 s at 270 °C. Such large change of welding time does not exist for the cases shown in Figure 9a.

Figure 10b corresponds to a rapid, steady cooling of the thermoplastic from 270 down to 250 °C in 10 s. The general trend among the models is similar to that noted in the case of AS4/PEEK, namely that the models of Bastien and Gillespie and of Sonmez and Hahn imply a slower healing development with respect to the exact solution during heating, and a rapid degree of healing evolution during cooling. Figure 10a shows that the time for complete welding, as predicted using Bastien and Gillespie's model, is larger than the exact solution by a factor of over 2. On the other hand, the welding time corresponding to the cooling schedule is considered underpredicted by the model of Bastien and Gillespie, by a factor of nearly 3.7. A significant deviation from the exact solution is also noted in the model of Sonmez and Hahn,[16] albeit to a lesser extent relative to the error introduced by the Bastien and Gillespie model.

Figure 11 presents comparison of the models for nonisothermal thermal histories encountered during actual processing of thermoplastic composites. The temperature variation in Figure 11a corresponds to a resistance welding of NCS/PEI reported by Bastien and Gillespie,[14] and consists of a heating segment followed by a cool down. Before the glass transition point of 230 °C is reached, all the models predict 0 degree of healing. However, significant differences are seen among the models as the resistance welding process progresses. Bastien and Gillespie's model predicts that the final degree of healing for this thermal history is only about 50%, while the other two models predict complete healing which is reached near the end of the heating segment of the temperature cycles. The model of Sonmez and Hahn matches the exact solution closely (within 10%) in terms of the total welding time for the particular temperature cycle and the welding time of NCS/PEI.

Figure 11b compares the models for AS4/PEKK subject to a temperature history in a thermoplastic tow-placement process reported by Pitchumani et al.[5] The welding time of AS4/PEKK was measured as described in the previous section, and is given in eq 25. The temperature profile has two heating and cooling cycles corresponding to the exposure of the material to two hot gas torches. In all the model predictions, the

degree of healing is seen to increase rapidly within the heating zones, while the healing rate is slower within the cooling zones. However, the degree of healing evolution shows large deviations among the models. At the end of the temperature cycle shown, the exact solution predicts a 47% degree of healing, relative to about 24% and 38% given by the models of Bastien and Gillespie and of Sonmez and Hahn, respectively.

The foregoing discussion pertained to a comparison of the available models with the exact solution for nonisothermal healing developed in this work. Experimental validation of the nonisothermal model was examined using the strength measurements on two thermoplastic materials—AS4/PEEK and AS4/PEKK ribbons. Lap shear specimens made of these materials were fabricated via fusion bonding in a hot press, as described previously. The specimens were tested under uniaxial tension to determine the breaking strength of the interface. The measured interlaminar shear strength values were normalized with respect to the maximum strength, σ_∞, to get the degree of healing. Specimens were fabricated at different nonisothermal schedules and for different duration within each schedule as tabulated in Table 2. Testing of these specimens yielded the degree of healing evolution with time, for each temperature schedule.

Figure 12 shows the degree of healing development of AS4/PEEK with time under the nonisothermal temperature conditions given by tests 1−3 in Table 2. The temperature-dependent welding time in eq 26 was used in the model predictions. The solid lines denote the predictions of the current model and the symbols with the error bars represent the experimental data. The dashed and the chain-dotted lines in the plot correspond to the other two models, as identified, and are included for comparison. As the temperature gradient decreases from part a to part c in Figure 12, the healing development expectedly slows down. Overall, the current model reveals good agreement with the experimental data for all the nonisothermal cycles and through the entire healing process. The predictions of the degree of healing by the models of Bastien and Gillespie and of Sonmez and Hahn fall below those of the current model and are consistent with the trend seen in Figures 9 and 10 for positive temperature ramps.

Further validation of the model was investigated using data on AS4/PEKK thermoplastic ribbons. Figure 13 shows the degree of healing evolution of the AS4/PEKK material at nonisothermal processing conditions corresponding to temperature schedules labeled tests 4−6 in Table 2. The welding time expression given by eq 25 was used in the model predictions, which are indicated by the solid, dashed, and chain-dashed lines. As in Figure 12, the symbols denote experimental data along with their error bars. The current model predictions on the degree of healing development with time are seen to be in close agreement with the experimental data for all the thermal histories considered. Furthermore, the models of Bastien and Gillespie and of Sonmez and Hahn predict a slower evolution of the healing.

Figure 13 reveals that the three model predictions move closer as the temperature ramp decreases in magnitude (Figure 13a−c). The same trend is also evident in Figure 12a−c, for AS4/PEEK. The observed trend is expected since the limit of a zero ramp denotes an isothermal condition for which all the three models are identical to the isothermal reptation model (eq 10).

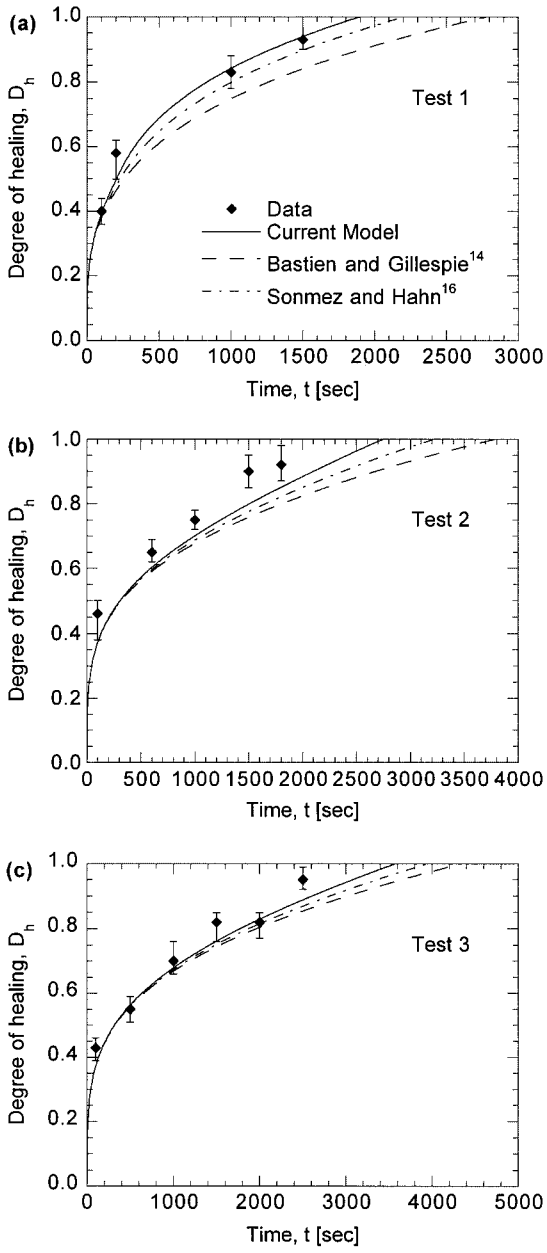

Figure 12. Validation of the nonisothermal healing model (eq 24**)** with experimental data on AS4/PEEK prepreg tows. Tests 1, 2, and 3 denote the temperature cycles in Table 2.

For the cases involving smaller temperature ramps, therefore, all the models are seen to compare reasonably well with experimental data. However, fabrication of thermoplastic and thermoplastic-matrix composite products based on techniques such as resistance welding, tow placement, or tape laying are highly nonisothermal involving rapid heating and cooling, for which the use of the models by Bastien and Gillespie or by Sonmez and Hahn could lead to errors as demonstrated in Figure 11.

The results presented in this section elucidate the nonisothermal healing process for various temperature histories and for different thermoplastic materials. The discussion in this paper focused on healing by assuming complete intimate contact at the interface. The nonisothermal healing model can be coupled with heat transfer and intimate contact models,[4−9] to obtain the interlaminar bond strength evolution during fabrication processes. Although not discussed in this article, the

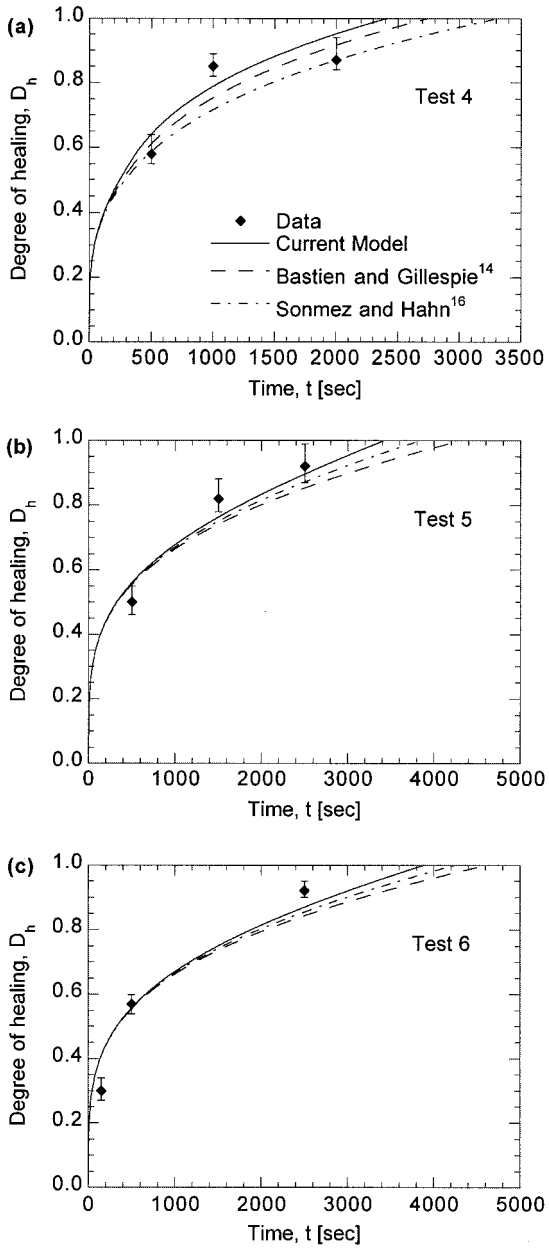

Figure 13. Validation of the nonisothermal healing model (eq 24) with experimental data on AS4/PEKK prepreg tows. Tests 4, 5, and 6 denote the temperature cycles in Table 2.

formulation of the nonisothermal reptation process and the exact solution for the minor chain length growth with time (eq 23) can be used to obtain the interfacial toughness development during processing. The toughness scales linearly with the minor chain length[14] and similar to the degree of healing based on interfacial strength defined previously, eq 4, a degree of healing, D_h^*, based on interfacial toughness may be defined as the ratio of the instantaneous toughness, G, to the maximum realizable toughness, G_∞. Using the expression for the minor chain length, l, from eq 23, the degree of healing based on interfacial toughness, D_h^* takes the form

$$D_h^* = \frac{G}{G_\infty} = \frac{l}{L_w} = \left[\int_0^t \frac{1}{t_w}\,dt\right]^{1/2} \qquad (27)$$

where t_w is the temperature-dependent welding time. The evaluation of D_h^* for a given temperature history is relatively straightforward, and the exploration of the toughness-based degree of healing evolution under nonisothermal conditions is left as an exercise to the interested reader.

5. Conclusions

A nonisothermal model of healing development during thermoplastic fusion bonding was developed based on first principles formulation of the polymer reptation process. An analytical solution was derived for the interlaminar strength development expressed in terms of a degree of healing, as a function of time and temperature. Parametric studies were presented to show the effects of temperature history on the degree of healing evolution with time. Experimental validation of the model was presented using measured interfacial strength data on different thermoplastic materials and processing conditions. The nonisothermal healing model was compared with the models of Bastien and Gillespie[14] and of Sonmez and Hahn[16] which are based on ad hoc extensions of the isothermal reptation model. It was shown that depending upon the nonisothermal history, the models of Bastien and Gillespie and of Sonmez and Hahn could yield considerably different estimates of the healing behavior, particularly for the conditions encountered during actual materials processing. For those cases involving smaller temperature gradients, which are therefore close to isothermal conditions, the models by Bastien and Gillespie and by Sonmez and Hahn were seen to be close to the exact solution presented in this study. The application of the analytical solution to prediction of interlaminar toughness was also discussed. The primary contribution of the work is that of providing a rigorous mathematical treatment and analysis of the nonisothermal healing process. The analytical model presented in this paper offers a reliable basis for prediction of interlaminar bonding development during thermoplastic materials processing.

Acknowledgment. The work reported in this paper was funded by the National Science Foundation (Grant No. CTS-9912093). AS4/PEEK and AS4/PEKK materials used in the experiments were provided by Cytec Fiberite, Inc. We gratefully acknowledge their support.

Nomenclature

D = reptation diffusion coefficient, m^2/s
D_0 = isothermal reptation diffusion coefficient at temperature T_0, m^2/s
D_h = degree of healing based on interfacial strength
D_h^* = degree of healing based on interfacial toughness
f = function defined in the model development for brevity (eq 22)
L = total length of a polymer chain, m
L_w = the length of a minor chain at the welding time, t_w, m
l = instantaneous minor chain length, m
M = polymer molecular weight, kg/kmol
P = probability density function, m^{-1}
$\hat{P}$ = Fourier transformation of the probability density function
$\hat{P}_0$ = Fourier transformation of the intial condition
s = curvilinear coordinate along the encompassing tube, m
T = temperature, K
t = time, s
t_R = reptation time of a thermoplastic material, s
t_w = welding time of a thermoplastic material, s

Greek Symbols

χ = interpenetration distance, m
χ_∞ = maximum interpenetration distance, m
χ_w = interpenetration distance at the welding time, t_w, m
δ = Dirac delta function, m^{-1}
σ = interlaminar bond strength, MPa
σ_∞ = ultimate interlaminar bond strength, MPa
ω = Fourier transformation variable in the frequency domain, m^{-1}

References and Notes

(1) Wool, R. P.; Yuan, B. L.; McGarel, O. J. *Polym. Eng. Sci.* **1989**, *29*, 1340−1367.
(2) Wool, R. P.; O'Connor, K. M. *J. Appl. Phys.* **1981**, *52*, 5953−5963.
(3) Kim, Y. H.; Wool, R. P. *Macromolecules* **1983**, *16*, 1115−1120.
(4) Lee, W. I.; Springer, G. S. *J. Compos. Mater.* **1987**, *21*, 1017−1055.
(5) Pitchumani, R.; Ranganathan, S.; Don, R. C.; Gillespie, J. W., Jr.; Lamontia, M. A. *Int. J. Heat Mass Transfer* **1996**, *39*, 1883−1897.
(6) Butler, C. A.; McCullough, R. L.; Pitchumani, R.; Gillespie, J. W., Jr. *J. Thermoplast. Compos. Mater.* **1998**, *11*, 338−363.
(7) Dara, P. H.; Loos, A. C. *Thermoplastic Matrix Composite Processing Model*; Virginia Polytechnic Institute Report CCMS-85-10; Virginia Polytechnic Institute: Hampton, VA, 1985.
(8) Yang, F.; Pitchumani, R. *J. Mater. Sci.* **2001**, *36*, 4661−4671.
(9) Yang, F.; Pitchumani, R. *Polym. Eng. Sci.* **2002**, *42*, 424−438.
(10) deGennes, P. G. *J. Chem. Phys.* **1971**, *55*, 572−579.
(11) Prager, S.; Tirrell, M. *J. Chem. Phys.* **1981**, *75*, 5194−5198.
(12) Bousmina, M.; Qiu, H.; Grmela, M.; Klemberg-Sapieha, J. E. *Macromolecules* **1998**, *31*, 8273−8280.
(13) Doi, M.; Edwards, S. F. *The Theory of Polymer Dynamics*; Clarendon Press: Oxford, U.K., 1986.
(14) Bastien, L. J.; Gillespie, J. W., Jr. *Polym. Eng. Sci.* **1991**, *31*, 1720−1730.
(15) Ageorges, C.; Ye, L.; Hou M. *Composites: Part A* **2001**, *32*, 839−857.
(16) Sonmez, F. O.; Hahn, H. T. *J. Thermoplas. Compos. Mater.* **1997**, *10*, 543−572.
(17) Wool, R. P. *Polymer Interfaces, Structure and Strength*, Hanser Publishers: Munich, Germany, Vienna, and New York, 1995; pp 74−81.
(18) Macosko, C. W. In *Rheology Principles, Measurements, and Applications*; Wiley-VCH: New York, 1994 pp 502−505.
(19) Qiu, H.; Bousmina, M. *J. Rheol.* **1999**, *43*, 551−568.
(20) Qiu, H.; Bousmina, M. *Macromolecules* **2000**, *33*, 6588−6594.
(21) Kreyszig, E. In *Advanced Engineering Mathematics*, 6th ed.; Wiley: New York, 1988.
(22) Steiner, K. V.; Bauer, B. M.; Pitchumani, R.; Gillespie, J. W., Jr. In *Proc. 40th Int. SAMPE Symp. Exhib.* **1995**, 1550−1559.

MA010858O